Concentration and excitation effects on the exciton dynamics of poly(3-hexylthiophene)/PbS quantum dot blend films

2013 Nanotechnology 24 235707

(http://iopscience.iop.org/0957-4484/24/23/235707)

Nanotechnology **24** (2013) 235707 (8pp) doi:10.1088/0957-4484/24/23/235707

Concentration and excitation effects on the exciton dynamics of poly(3-hexylthiophene)/PbS quantum dot blend films

D Tsokkou[1], G Itskos[2], S Choulis[3], M Yarema[4], W Heiss[4] and A Othonos[1]

[1] Department of Physics, Research Center of Ultrafast Science, University of Cyprus, Nicosia 1678, Cyprus
[2] Department of Physics, Experimental Condensed Matter Physics Laboratory, University of Cyprus, Nicosia 1678, Cyprus
[3] Molecular Electronics and Photonics Research Unit, Department of Mechanical Engineering and Materials Science and Engineering, Cyprus University of Technology, Limassol 3603, Cyprus
[4] Institute of Semiconductor and Solid State Physics, University of Linz, Linz A-4040, Austria

E-mail: tsokkou.demetra@ucy.ac.cy

Received 7 February 2013, in final form 27 March 2013
Published 15 May 2013
Online at stacks.iop.org/Nano/24/235707

Abstract
The dynamics of photoexcitations in hybrid blends of poly(3-hexylthiophene) (P3HT) conjugated polymer donor and oleic-acid capped lead sulfide (PbS) quantum dot (QD) acceptors of different concentrations—for light harvesting applications—were investigated using time-resolved transmission and photoluminescence spectroscopies. Following excitation at 400 nm and probing in the 500–1000 nm region, we find that geminate excitation recombination in the blend of P3HT/PbS QDs dominates the transient decays at sub-ns times while intermaterial interactions such as charge transfer processes appear at longer times in the 1–50 ns regime. For the hybrid blend films with lower QD concentrations (<67% wt), polymer exciton recombination dominates the overall transient absorption signal. For higher QD contents, QD state relaxation effects become visible. Excitation density studies reveal the presence of linear exciton relaxation effects in the P3HT region while carrier decay for films with high PbS QD concentration is influenced by QD Auger recombination. Time-resolved luminescence shows that electron transfer from the P3HT/PbS QDs appears relatively inefficient in comparison to the geminate recombination, while hole transfer competes favorably to intrinsic QD recombination.

(Some figures may appear in colour only in the online journal)

1. Introduction

The demonstration of bulk heterojunction (BHJ) blends based on the mixing of two or more solution processed materials with suitable energy level alignment was a crucial step towards efficient organic and hybrid light harvesting devices [1–4]. Typically in such blends, a highly absorbent conjugated polymer like poly(3-hexylthiophene) (P3HT) is used as the electron donor material and a fullerene, i.e. [6,6]-phenyl-C61-butyric acid methyl ester (PCBM), plays the role of the electron acceptor material [5–7]. Such devices have shown remarkable progress, demonstrating milestone solar cell efficiencies [8] and high performance photodiodes fabricated via large area coating techniques [9].

To further improve the performance of such devices there are a few more operational drawbacks that need to be overcome. For solar cells, it is important to increase the spectral overlap of the active layer absorption with

the solar emission. For sensors, a plethora of applications require operation in infrared. Both of the above require the use of low band gap material. A promising pathway towards this direction is the replacement of the fullerene electron acceptor by quantum-confined tunable, colloidal quantum dots (QDs) [10–14]. The most promising results on IR hybrid light harvesting have been demonstrated using lead chalcogenide dots, owing to their highly attractive electronic properties [15]. Rauch *et al* have reported infrared photodiodes based on blends of oleic-acid capped PbS QDs with P3HT and PCBM with high quantum efficiencies up to 50% and spectral sensitivity up to 1800 nm [16], while hybrid QD/polymer solar cells reaching power conversion efficiencies up to 4% have been demonstrated [17, 18].

To further optimize device performance, it is essential that a thorough understanding of the photophysics of such hybrid blends is achieved. Despite a number of reported studies [19–22] there are aspects of the polymer–QD interaction that are worth further investigation. In previous work by our group, photoluminescence (PL) and transient transmission spectroscopy methods were used to investigate ternaries of P3HT:PCBM:oleic-acid capped PbS QDs [23]. Information on the dissociation of excitons and intermaterial charge transfer processes has been obtained; the results were in close agreement with concurrent studies of similar ternary films based on time-resolved photoluminescence (TR-PL) [24]. To extend our studies, we report here a study of binary composites of P3HT:oleic-acid capped PbS QDs with a view to assessing further the influence of two parameters on the blends' photophysics: concentration and excitation density. Femtosecond non-degenerate transmission spectroscopy is used as the main experimental tool to probe exciton dynamics, supplemented by TR-PL. We investigate the impact of nanocrystal concentration and the influence of QD Auger recombination on the polymer exciton dynamics by monitoring the evolution of the transient signal as a function of probing wavelength and excitation fluence. We also observe that geminate recombination in the polymer dominates exciton recombination up to 500 ps with intermaterial charge transfer processes appearing at longer, ns ranges.

2. Experimental details

2.1. Sample preparation

Regioregular P3HT and C60-PCBM were purchased from Rieke Metals and Solenne respectively, while oleic-acid capped PbS nanocrystals were synthesized according to methods reported in the literature [25]. We opted to use oleic-acid capped PbS QDs due their good material quality, stability and homogeneity, which suit a systematic spectroscopic study. The investigated films were binary blends of P3HT and PbS QDs mixed with weight ratios of 1:1, 1:2, 1:4 and 1:8 (wt%) along with reference samples of pristine P3HT, QDs and P3HT:PCBM 1:1 films. The polymer and QDs were dissolved in chlorobenzene under nitrogen atmosphere and deposited on quartz substrates with a size of 1 $\times$ 1 cm^2 via a doctor blade. Although different samples with PbS QDs in the range of 3–5 nm were fabricated, here we discuss blends based on the smaller ($\sim$3 nm) dots as such films showed superior optical quality with no visible quantum dot aggregation within the polymer material. The film thickness of all samples was controlled to be approximately the same, in the range of 300–400 nm as verified by a Dektak profilometer.

2.2. Time-resolved spectroscopy experiments

To perform time-resolved transmission spectroscopy measurements, an ultrafast amplifier laser system was used. The mode-locked ultrashort pulses from the oscillator (Tsunami, Spectra Physics) with central wavelength at 800 nm and a time duration of $\sim$100 fs served as the seed for the regenerative amplifier (Spitfire, Spectra Physics) to produce 120 fs output pulses of 1 mJ/pulse with a 1 kHz repetition rate. Measurements were carried out using a typical pump–probe optical setup in a non-collinear configuration. A nonlinear second harmonic BBO crystal was used to obtain excitation pulses at 400 nm. In addition, white light continuum pulses in the region between 500 and 1100 nm were generated in a sapphire crystal and used as the probe pulses. The energy of the probe beam is sufficiently small to be considered as a perturbation for the examined system and is at least three orders of magnitude weaker than that of the pump beam. The probed wavelength was selected by appropriate bandpass filters. The time delay between the two pulses was achieved via a computer controlled translation stage with special resolution of 0.1 μm. During the experiments the samples were mounted into a nitrogen flow through cell and kept under nitrogen atmosphere.

TR-PL was employed to complement the pump–probe measurements, extending our investigations to longer times of up to 50 ns. PL decays were measured by a spectrometer equipped with a visible photomultiplier tube using the time-correlated single-photon counting (TCSPC) technique. Excitation was provided by a 1 MHz, 375 nm picosecond laser diode. The system exhibited a time-resolution of 50 ps after reconvolution with the instrument response function. The incident laser beam was deliberately kept at moderate to low powers of 1–0.1 mW, comparable to those used in transient absorption experiments, and focused to relatively large spots on the film surfaces of 1–2 mm^2 to allow better sample averaging. All PL experiments were carried in vacuum conditions ($\sim 10^{-3}$ Torr).

3. Experimental results and discussion

3.1. Absorbance measurements

The absorbance spectra of pristine P3HT, PbS QD and binary P3HT:PbS QD binary samples, along with the PL spectrum of P3HT, are displayed in figure 1. For clarification, a magnified graph of the absorbance in the case of hybrid samples, at the region between 650 and 1200 nm, is included as an inset. Also, the energy band offsets of the two components are depicted, as an inset on the right side of figure 1, which show that electron transfer from the polymer to the QDs and hole transfer from the QDs to the polymer states may occur after photoexcitation [26].

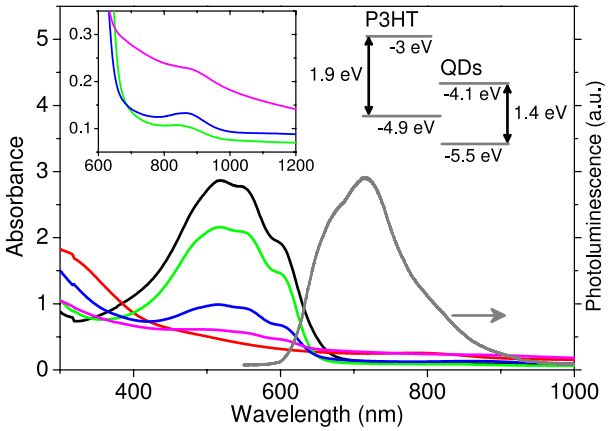

Figure 1. Steady state absorbance spectra of pristine P3HT film (black line), pure PbS QD (red line) and hybrid binary P3HT:PbS QD films with weight ratio 1:1 (green line), 1:4 (blue line) and 1:8 (violet line). In addition, the PL spectrum of P3HT film (gray line) is shown. In the inset of the figure, a magnified graph of the absorption spectra of hybrid samples in the near-infrared region and a simplified scheme of the hybrid samples' band diagram are included.

In the visible region, the characteristic π–π^* absorption band of the P3HT is observed [27], being responsible for most of the light absorption up to the P3HT band edge. There are no significant variations in the spectral characteristics of the polymer absorbance or luminescence in the hybrid samples relative to those of P3HT, even for high QD loadings, which can be interpreted as a sign of rather weak structural and electronic interactions of the blend components. In the near-infrared region, the QD ground state transition is identified by an absorption peak at ∼880 nm, more visible in the inset of figure 1.

3.2. Carrier dynamics in hybrid P3HT:PbS QD films

Time-resolved experiments were initially performed on the pristine P3HT and PbS QD films, to elucidate the contribution from each component to the detected signal by the hybrids. Non-degenerate transient measurements were carried out using excitation pulses at 400 nm, with time duration of ∼150 fs, pump fluence of ∼0.5 mJ cm^{-2} and various probing pulses ranging between 500 and 1000 nm. The normalized experimental data of P3HT film and QDs are shown in figures 2(a) and (b), respectively. Measurements were performed for times up to 500 ps, however only the first 200 ps are shown here for clarity. In addition, the maximum transient signal as a function of probing wavelength is displayed in the inset of each figure.

Photoexcitation of regioregular P3HT at 400 nm (E = 3.1 eV) results mainly in the photogeneration of singlet excitons, however fractions of polarons and polaron pairs are also present [28, 29]. Transients across our probing range can be adequately described by 3-exponentials with two decays of sub- and few ps timescales and a significantly longer decay of hundreds of ps identified as the P3HT exciton lifetime, as described in [23]. For probes shorter

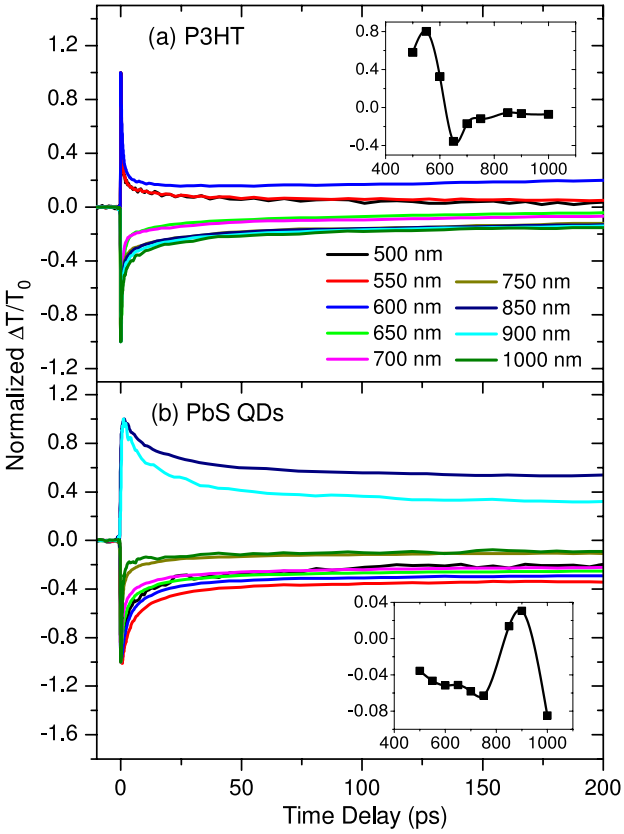

Figure 2. Non-degenerate transient normalized transmission change signal of (a) pristine P3HT film and (b) pure PbS QDs using excitation pulses at 400 nm, excitation fluence of 0.5 mJ cm^{-2} and probing pulses in the spectral region 500–1000 nm. In the inset of each figure, the maximum transmission change as a function of probing wavelength is included.

than 600 nm, positive transient signals are assigned to the photobleaching of the singlet exciton states. It should be mentioned that in our data a distinct behavior, with a much slower signal relaxation at 600 nm relative to that at 500 and 550 nm, is observed, which has not been reported by earlier studies. This indicates the presence of long lived excitations in the polymer, possibly polarons; it is unlikely that the signal is due to exciton fluorescence as no significant P3HT emission occurs at 600 nm (shown in figure 1). Further measurements are needed to clarify the origin of this peculiar behavior. Negative transient signals for longer wavelengths are related to photoinduced absorption to excited states. Based on previous studies, the signal around 650 nm is attributed to polaron pairs [28, 29] while the slow relaxation at longer probes (∼1000 nm) has been assigned to polarons [29]. The absence of stimulated emission in the spectral region of P3HT fluorescence, namely ∼650–750 nm, is attributed to P3HT interchain interactions [28, 29].

A significantly different behavior is obtained in the PbS QD films upon photoexcitation at 400 nm, as seen in figure 2(b). The spectral range of probing pulses gives the ability to study both intraband and interband QD transitions. As demonstrated in figure 2(b) (and in the inset of figure 2(b)), a negative differential transmission signal

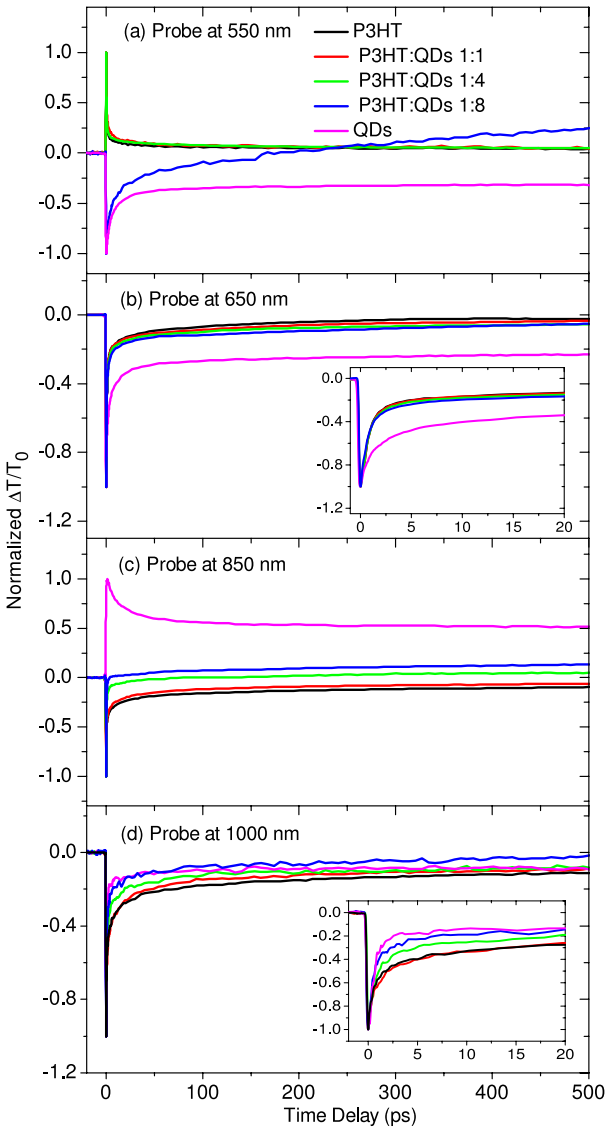

Figure 3. Normalized transmission change measurements for the hybrid binary P3HT:QD films with different weight ratios, pristine P3HT film and pure PbS QDs using excitation pulses at 400 nm and different probing pulses at (a) 550 nm, (b) 650 nm, (c) 850 nm and (d) 1000 nm. In the insets of figures (b) and (d), the normalized data for the first 20 ps are shown.

is evident for most probing wavelengths, associated with photoinduced absorption to higher lying excited states. The positive transmission change in the spectral region between 850 and 900 nm is attributed to state filling effects of the QD quantized states, consistent with the results of the steady state transmission measurements. Slow decays of ns timescales are observed, consistent with previous studies of photoexcitations in PbS QDs [30].

Typical decays from blend films with different polymer–QD ratios along with those of the reference films at several different probing wavelengths from visible to near-IR, are presented in figure 3. The behavior of the samples shows different trends at the following four probe ranges: (a) 500–600 nm, (b) 650–750 nm, (c) 850–900 nm and (d) 1000–1100 nm, displayed respectively in the four graphs of figure 3.

Following photoexcitation of the hybrid films with low QD concentration at 400 nm, the majority of primary carrier generation occurs in the polymer, because it exhibits a higher absorption at 400 nm compared to that from PbS QDs. However, the QD absorbance as extracted from the steady state transmission measurements is not negligible and a number of carriers are expected to be generated in the QDs.

For the first spectral region, which coincides with the P3HT exciton ground state, the long transient decay in the 1:1 and 1:4 wt% films is identical to that of the pristine polymer. Therefore, we can safely conclude that (i) the measurements probe mainly polymer states, (ii) geminate recombination in the polymer dominates with no significant polymer–QD interaction effects, i.e. charge transfer, directly visible in the polymer exciton relaxation. On high QD loadings of 80 wt% QDs, the transient behavior changes. A negative differential transmission signal is detected at times up to 200 ps, in agreement with the dynamics of the pristine PbS QD films, while the signal becomes positive at longer times. It can be concluded that at high QD content, excitations are predominantly photogenerated in QDs which are responsible for the long photobleaching observed. However at times longer than 200 ps, polymer relaxation effects appear.

At the spectral region between 650 and 750 nm, coincident with the P3HT fluorescence (figure 3(b) and its inset), the QDs even at high concentrations influence negligibly the polymer exciton dynamics. Geminate P3HT exciton recombination is predominantly probed and found to be dominated by the relaxation channel occurring at ultrafast sub-ps scales; the relaxation across this range has been previously ascribed to recombination of polaron pairs [28, 29].

At longer wavelengths of 850 nm that coincide with the QD interband electronic transitions (figure 3(c)) a negative signal is measured for all examined hybrid samples at times near zero, similar to that for the polymer film. For films of low QD content, the signal is dominated by polymer excitations, most probably polarons, as indicated by previous studies. As the QD content increases the signal recovery becomes progressively faster, while for the higher QD content sample the negative signal becomes positive, within ∼3 ps, due to QD state filling effects. At even longer probing wavelengths between 1000 and 1100 nm (figure 3(d)) P3HT polaron and QD interband absorption effects are simultaneously detected. From the inset of figure 3(d), it is evident that the decays become progressively faster as the QD concentration increases and systematically approach the behavior of the pristine QD sample.

The pump–probe measurements were supplemented by TR-PL experiments to probe possible photoinduced electron transfer processes from the polymer to the PbS QDs. In all comparative measurements the excitation laser density was normalized to the absorbance of the films at 375 nm to photoexcite an approximately equal number of excitons in all pristine and blend samples. Figure 4 shows comparative PL decays from the pristine P3HT film along with three

Table 1. PL decay lifetimes, peak intensity quenching and electron transfer rate parameters.

Sample	Peak intensity quench. (±5%)	Lifetime (±10 ps)	Electron transfer time (ns)
P3HT	—	445	—
1:1	24	375	2.40
1:2	40	350	1.60
1:4	78	320	1.05
P3HT:PCBM	94	240	0.50

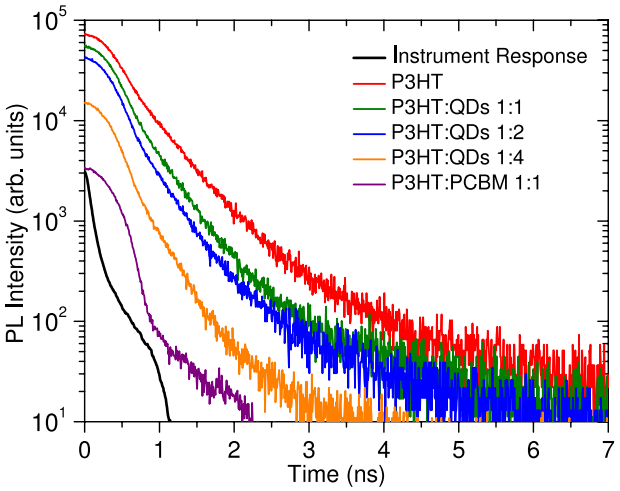

Figure 4. Comparative PL decays at logarithmic scale of P3HT, P3HT:PbS QD and P3HT:PCBM films, monitoring the main P3HT vibronic at 715 nm.

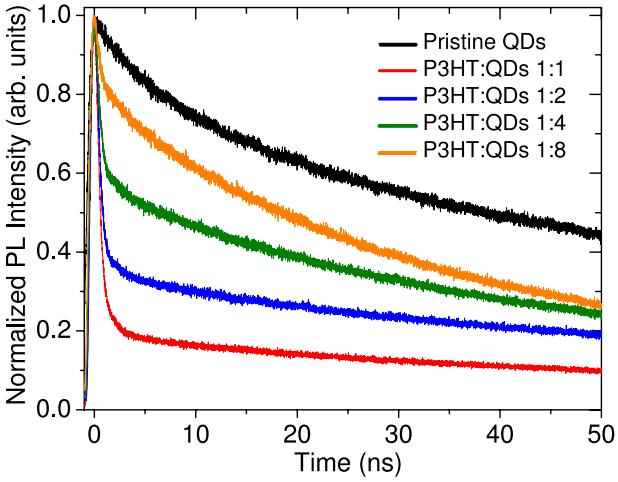

Figure 5. Normalized PL dynamics of QD emission at pristine and blend P3HT:QD films with different polymer–QD ratios monitoring the PL peak at 1000 nm.

QD-blends where the QD to P3HT ratio is systematically varied. The decays are recorded by monitoring the main polymer vibronic emission peak at ∼715 nm, however similar trends are obtained by monitoring the weaker P3HT vibronic at ∼675 nm (see figure 1). For comparison, the decay from a 1:1 wt% P3HT:PCBM blend film is also displayed.

As observed in figure 4, the blends exhibit quenching of both PL peak intensity and emission lifetime relative to the pristine film. The quenching is dependent on the QD to P3HT ratio and is predominantly attributed to electron transfer processes from the P3HT to the PbS QD states. The PL decays, especially those of the blend films, exhibit a distribution of decaying lifetimes. For the purpose of the present discussion, a sufficient decay description can be obtained using a single, effective lifetime per sample. The associated emission quenching factors and PL lifetimes (rates) from the studied samples are listed in table 1. Electron transfer rates can be obtained by the difference between the blend and the pristine exciton recombination rates. Electron transfer to the QDs, as witnessed by both the intensity and lifetime quenching, is relatively slow (∼1–2.5 ns) compared to pristine polymer exciton recombination (∼0.45 ns). Even at high QD loadings (80 wt%) exciton quenching appears significantly less efficient than that observed in a conventional 1:1 P3HT:PCBM blend. As mentioned in previous work, the inhibition of charge transfer can be predominantly attributed to the presence of the long insulating oleic-acid ligands [23, 24].

The influence of excitation density on the TR-PL dynamics was also studied (not shown). The measurements show that the P3HT PL lifetimes in both pristine and blend films exhibit negligible variations of the order of ∼10% and ∼5% respectively, upon variations of an order of magnitude in excitation density. This equivalently indicates that the electron transfer efficiency from P3HT to QDs is weakly dependent on excitation density.

We have also investigated whether hole transfer from the QDs to the P3HT occurs and whether such processes take place at timescales that can affect the pump–probe transient signals (i.e. up to 500 ps). To do this, time-resolved studies monitoring the QD emission peak at 1000 nm (∼1.24 eV) have been carried out. The summary of such measurements is shown in figure 5.

The pristine QD film shows an approximate monoexponential decay of ∼35 ns while blend films are described by double exponentials of the form

$$I(t) = I_1 e^{-\frac{t}{\tau_1}} + I_2 e^{-\frac{t}{\tau_2}}. \quad (1)$$

The contribution of each of the two time constants $\tau_{1,2}$ is quantified by its relative amplitude expressed as

$$A_{1,2} = \frac{I_{1,2}}{I_1 + I_2} \cdot 100\%. \quad (2)$$

The results are shown in table 2. The fittings consistently yield a sub-ns component, most probably due to Auger recombination, and a slower component, comparable to the

Table 2. PL decay fitting parameters in the region of QD emission and estimated hole transfer times.

Sample	τ_1 (ns)	A_1 (%)	τ_2 (ns)	A_2 (%)	τ^* (ns)	Hole transfer (ns)
QD	35	83	—	—	35	—
1:8	30	76	0.9	24	23	68.0
1:4	35	45	0.6	55	16	29.5
1:2	36	23	0.45	77	8.5	11.0
1:1	34	12	0.5	88	4.5	5.0

pristine QD lifetime. A systematic quenching of the PL lifetime with P3HT content is clearly visible in figure 5. The quenching of PL lifetime can be predominantly attributed to hole transfer processes from the QD electronic states to the P3HT. In the fitting parameters of table 2, the quenching is manifested by an increase in the relative contribution of the fast over the slow decay component, with the former dominating the decay for blends with large enough P3HT content. To obtain a quantitative measure of the hole transfer time, an effective QD lifetime is defined in the blends as

$$\tau^* = A_1\tau_1 + A_2\tau_2. \quad (3)$$

Using a similar methodology to that used to obtain the electron transfer rates, hole transfer times of ∼5, 11, 30 and 68 ns for the 1:1, 1:2, 1:4 and 1:8 blends are obtained, respectively. It is noted that such hole transfer processes were studied before [23, 24], however the influence of blend concentration on the transfer efficiency remained rather unexplored. Comparison of the transfer times with the pristine QD lifetime indicates that unlike the findings in the polymer region, hole transfer competes favorably to intrinsic QD recombination for the blends of 1:1, 1:2 and even 1:4. However the hole transfer occurs at timescales of several ns and thus it does not influence directly the significantly faster transients observed in the pump–probe experiments.

3.3. Intensity-dependent transient transmission measurements in hybrid P3HT:PbS QD films

The influence of pump fluence on the excitation dynamics is often an unexplored parameter in reported spectroscopic studies of BHJs. Figures 6(a) and (b) present normalized transmission transients for the pristine P3HT and the hybrid 1:1 wt% P3HT:PbS QD films respectively, over a wide range of excitation pump fluences. A probe of 600 nm was used to directly probe the P3HT singlet exciton states.

In the pristine P3HT film, the fast components of the differential transmission become faster as the pump fluence increases, while the longer component remains almost constant up to 500 ps. Such behavior is expected when bimolecular recombination such as exciton–exciton annihilation takes place. However, the linear dependence of the maximum differential transmission as a function of the pump fluence, seen in the inset of figure 6(a), shows that the relaxation in P3HT is governed by monomolecular exciton processes. Similar results are obtained from the 1:1 blend, i.e. a linear dependence of the fast relaxation rate on fluence and an insensitivity of the long decay channel on excitation, which also confirms that the polymer contribution dominates

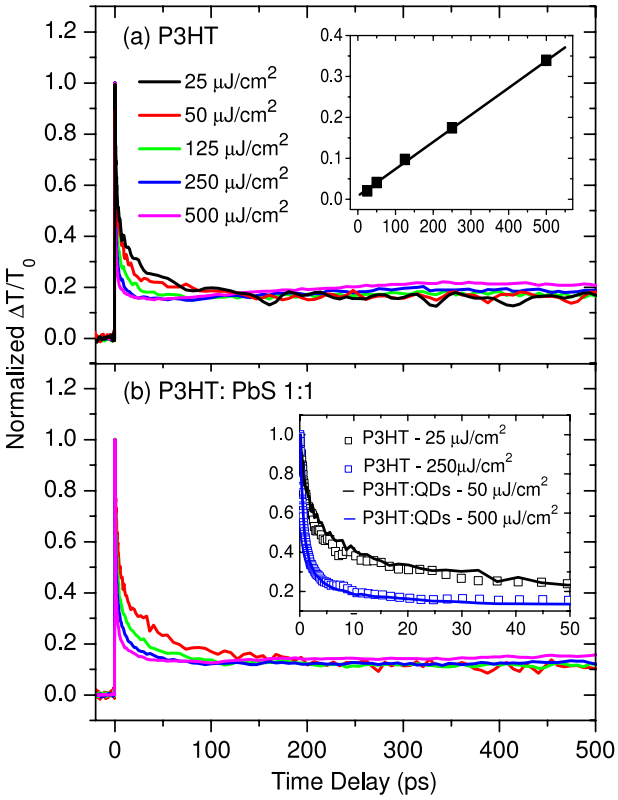

Figure 6. Temporal evolution of normalized transmission change for (a) pristine P3HT and (b) 1:1 wt% P3HT:PbS QDs using excitation pulses at 400 nm, probing pulses at 600 nm and different excitation fluences. In the inset of figure 6(a), the maximum transmission change as a function of the pump fluence is shown. In addition, the normalized transmission data for P3HT (dots) and 1:1 wt% P3HT:PbS QDs (lines) for different pump fluences for times up to 50 ps are seen in the inset of figure 6(b).

the temporal signal evolution. Remarkably, as is displayed in the inset of figure 6(b), for similar photoexcited carrier densities in both samples, the signal evolution does not exhibit any significant changes. This is indicative that no intermaterial interaction effects, such as interface carrier trapping or photoinduced charge transfer, occur at such early times, in accordance with the findings of TR-PL measurements.

The effect of pump fluence is more evident on the high content QD samples of 1:4 and 1:8 wt% P3HT:PbS QDs, and the reference QD films, whose decays for various excitations are shown in figures 7(a), (b) and (c) respectively. Initially, it is seen that the temporal decay from the PbS QDs becomes faster as a function of pump fluence. The reduction in relaxation times is indicative that the primary relaxation channel probed is Auger recombination [31]. Unlike the

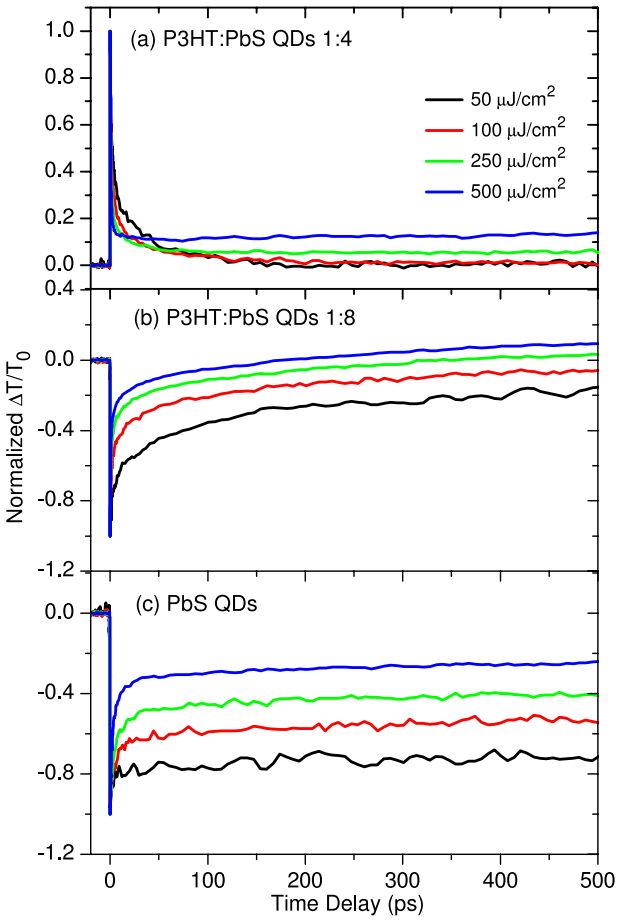

Figure 7. Excitation intensity dependent normalized transmission change measurements for (a) 1:4 wt% P3HT:PbS QDs, (b) 1:8 wt% P3HT:PbS QDs and (c) pure PbS QDs using excitation pulses at 400 nm, probing pulses at 600 nm and different excitation fluences in the range between 50 and 500 μJ cm^{-2}.

pristine polymer film and the 1:1 blend, the long decay component of the 1:4 film is intensity dependent, and rather unexpectedly becomes slower as the fluence increases. The modifications observed are a result of the simultaneous contributions to the overall signal from both composites and the presence of Auger recombination in QDs. At high pump fluences, the signal evolution for the 1:4 wt% hybrid film is mainly determined by the polymer contribution, since carriers in the QDs relax quickly to lower states due to Auger recombination. On the other hand, at low pump fluences Auger recombination becomes weak and the signal due to QD state effects also contributes to the overall signal.

The signal from the 1:8 wt% film (figure 7(b)) shows a negative sign, similar to that of the pristine QD films, which becomes faster as the pump fluence increases. This is also consistent with the presence of Auger recombination that efficiently replenishes the detected states allowing photoinduced absorption effects related to the polymer states to appear at longer times. It is noted that effects such as multiple exciton generation in the PbS QDs are not expected to have a significant contribution following photoexcitation at 400 nm, since they efficiently occur for pump photon energies larger than ∼2.5–3 times the QD energy band gap, while in our case the pump is at ∼2.25 times the QD energy gap [32, 33].

4. Conclusions

In conclusion, we have performed a detailed investigation of photoexcitation dynamics in binary bulk heterojunctions based on P3HT conjugated polymer donor and oleic-acid capped PbS QDs relevant to a range of light harvesting applications, using time-resolved transmission and luminescence techniques. Our study focused on the effects of blend composition and excitation fluence, in order to distinguish the role of each component in the overall transient signal. For the hybrid blends with low QD concentration, upon 400 nm excitation, primary photoexcitations occur in the conjugated polymer with a slight influence of the dynamics at longer wavelengths (≥850 nm) by QD carrier relaxation. More importantly, it is shown that pump–probe experiments probe predominantly conjugated polymer geminate recombination up to 500 ps, while no signal modifications due to intermaterial interaction effects are evident. Furthermore, excitation and relaxation for blends with high QD concentration involves contributions from both conjugated polymer and QDs with the contributions being strongly intensity dependent. Intermaterial charge transfer processes in P3HT/PbS QD blends appear at longer times, as verified by TR-PL measurements that allow measurement of electron and hole transfer times at timescales of 1 ns and 5 ns, respectively. The experiments thus verify that after mixing of P3HT and oleic-acid PbS QDs in various ratios and at various excitation fluences, electron transfer is relatively inefficient in comparison to geminate recombination. In contrast, hole transfer competes the intrinsic QD recombination that is of great importance for the operation of infrared detectors and solar cells based on ternary blends containing PbS QDs as sensitizers and separate electron and hole accepting materials.

Acknowledgments

This research work is partly supported by the Cyprus Research Promotion Foundation ('NEA ΥΠΟΔΟΜΗ/ΣΤΡΑΤΗ/0308/06') and by the Austrian Science Funds FWF (Project SFB IR ON).

References

[1] Sariciftci N S, Smilowitz L, Heeger A J and Wudl F 1992 *Science* **258** 1474
[2] Brabec C J, Gowrisanker S, Halls J J M, Laird D, Jia S and Williams S P 2010 *Adv. Mater.* **22** 3839
[3] Clarke T M and Durrant J R 2010 *Chem. Rev.* **110** 6736
[4] Piris J, Dykstra T E, Bakulin A A, Loosdrecht P H M, Knulst W, Trinh M T, Schins J M and Siebbeles L D A 2009 *J. Phys. Chem.* C **113** 14500
[5] Dennler G, Scharber M C and Brabec C J 2009 *Adv. Mater.* **21** 1323
[6] Dang M T, Hirsch L and Wantz G 2011 *Adv. Mater.* **23** 3597
[7] Al-Ibrahim M, Ambacher O, Sensfuss S and Gobsch G 2005 *Appl. Phys. Lett.* **86** 201120

[8] http://www.polyera.com/newsflash/polyera-achieves-world-record-organic-solar-cell-performance
[9] Tedde S F, Kern J, Sterzl T, Furst J, Lugli P and Hayden O 2009 *Nano Lett.* **9** 980
[10] Greenham N C, Peng X and Alivisatos A P 1996 *Phys. Rev.* B **54** 17628
[11] Huynh W U, Dittmer J J and Alivisatos A P 2002 *Science* **295** 2425
[12] Wright M and Uddin A 2012 *Sol. Energy Mater. Sol. Cells* **107** 87
[13] Saunders B and Turner M L 2008 *Adv. Colloid Interface Sci.* **138** 1
[14] Saunders B R 2012 *J. Colloid Interface Sci.* **369** 1
[15] Rogach A L, Eychmüller A, Hickey S G and Kershaw S V 2007 *Small* **3** 536
[16] Rauch T, Boberl M, Tedde S F, Furst J, Kovalenko M V, Hesser G N, Lemmer U, Heiss W and Hayden O 2009 *Nature Photon.* **3** 332
[17] Seo J, Cho M J, Lee D, Cartwright A N and Prasad P N 2011 *Adv. Mater.* **23** 3984
[18] Piliego C, Manca M, Kroon R, Yarema M, Szendrei K, Andersson M R, Heiss W and Loi M A 2009 *J. Mater. Chem.* **22** 24411
[19] Sun Z, Li J and Yan F 2012 *J. Mater. Chem.* **22** 21673
[20] Seo J, Kim S J, Kim W J, Singh R, Samoc M, Cartwright A N and Prasad P N 2009 *Nanotechnology* **20** 095202
[21] Guchhait A, Rath A K and Pal A J 2010 *Appl. Phys. Lett.* **96** 073505
[22] Noone K M, Subramaniyan S, Zhang Q, Cao G, Jenekhe S A and Ginger D S 2011 *J. Phys. Chem.* C **115** 24403
[23] Itskos G, Othonos A, Rauch T, Tedde S F, Hayden O, Kovalenko M V, Heiss W and Choulis S A 2011 *Adv. Energy Mater.* **1** 802
[24] Jarzab D, Szendrei K, Yarema M, Pichler S, Heiss W and Loi M A 2011 *Adv. Funct. Mater.* **21** 1988
[25] Hines M A and Scholes G D 2003 *Adv. Mater.* **15** 1844
[26] Gocalinska A *et al* 2010 *J. Phys. Chem. Lett.* **1** 1149
[27] Brown P J, Thomas D S, Kohler A, Wilson J S, Kim J-S, Ramsdale C M, Sirringhaus H and Friend R H 2003 *Phys. Rev.* B **67** 064203
[28] Jiang X M, Osterbacka R, Korovyanko O, An C P, Horovitz B, Janssen R A J and Vandeny Z V 2002 *Adv. Funct. Mater.* **12** 587
[29] Guo J, Ohkita H, Benten H and Ito S 2009 *J. Am. Chem. Soc.* **131** 16869
[30] Shen Q, Katayama K, Sawada T, Hachiya S and Toyoda T 2012 *Chem. Phys. Lett.* **542** 89
[31] Istrate E, Hoogland S, Sukhovatkin V, Levina L, Myrskog S, Smith P W E and Sargent E H 2008 *J. Phys. Chem.* B **112** 10
[32] Gesuele F, Sfeir M Y, Koh W-K, Murray C B, Heinz T F and Wong C W 2012 *Nano Lett.* **12** 2658
[33] Nootz G, Padilha L A, Levina L, Sukhovatkin V, Webster S, Brzozowski S, Sargent E H, Hagan D J and Stryland E W V 2011 *Phys. Rev.* B **83** 155302